Direct optical transitions at K- and H-point of Brillouin zone in bulk MoS_2, $MoSe_2$, WS_2, and WSe_2

J. Kopaczek, M. P. Polak, P. Scharoch, K. Wu, B. Chen, S. Tongay, and R. Kudrawiec

Citation: Journal of Applied Physics **119**, 235705 (2016); doi: 10.1063/1.4954157
View online: http://dx.doi.org/10.1063/1.4954157
View Table of Contents: http://aip.scitation.org/toc/jap/119/23
Published by the American Institute of Physics

JOURNAL OF APPLIED PHYSICS **119**, 235705 (2016)

Direct optical transitions at K- and H-point of Brillouin zone in bulk MoS_2, $MoSe_2$, WS_2, and WSe_2

J. Kopaczek,[1,a)] M. P. Polak,[1,a)] P. Scharoch,[1] K. Wu,[2] B. Chen,[2] S. Tongay,[2] and R. Kudrawiec[1,b)]
[1]*Faculty of Fundamental Problems of Technology, Wroclaw University of Technology, Wybrzeże Wyspiańskiego 27, 50-370 Wrocław, Poland*
[2]*School for Engineering of Matter, Transport and Energy, Arizona State University, Tempe, Arizona 85287, USA*

(Received 15 March 2016; accepted 5 June 2016; published online 21 June 2016)

Modulated reflectance (contactless electroreflectance (CER), photoreflectance (PR), and piezoreflectance (PzR)) has been applied to study direct optical transitions in bulk MoS_2, $MoSe_2$, WS_2, and WSe_2. In order to interpret optical transitions observed in CER, PR, and PzR spectra, the electronic band structure for the four crystals has been calculated from the first principles within the density functional theory for various points of Brillouin zone including K and H points. It is clearly shown that the electronic band structure at H point of Brillouin zone is very symmetric and similar to the electronic band structure at K point, and therefore, direct optical transitions at H point should be expected in modulated reflectance spectra besides the direct optical transitions at the K point of Brillouin zone. This prediction is confirmed by experimental studies of the electronic band structure of MoS_2, $MoSe_2$, WS_2, and WSe_2 crystals by CER, PR, and PzR spectroscopy, i.e., techniques which are very sensitive to critical points of Brillouin zone. For the four crystals besides the A transition at K point, an A_H transition at H point has been observed in CER, PR, and PzR spectra a few tens of meV above the A transition. The spectral difference between A and A_H transition has been found to be in a very good agreement with theoretical predictions. The second transition at the H point of Brillouin zone (B_H transition) overlaps spectrally with the B transition at K point because of small energy differences in the valence (conduction) band positions at H and K points. Therefore, an extra resonance which could be related to the B_H transition is not resolved in modulated reflectance spectra at room temperature for the four crystals. *Published by AIP Publishing.*
[http://dx.doi.org/10.1063/1.4954157]

I. INTRODUCTION

Transition metal dichalcogenides (TMDs), such as MoS_2, $MoSe_2$, WS_2, and WSe_2, have been very intensively investigated for the past few years since their electronic band structure and optical properties vary very strongly with the number of monolayers.[1–3] The electronic band structure of bulk TMDs (mainly MoS_2) has been investigated both in the past[4–11] and quite recently when researchers studied the evolution of the electronic band structure in these crystals with reduction of their sizes from a bulk regime through a few layers to a monolayer.[12–14] However, some issues for bulk materials are still unclear. One of them is the electronic band structure at the H point of the Brillouin zone and optical transitions at this point. The space group $P6_3/mmc$, to which all the studied crystals belong, has a Brillouin zone which is a hexagonal prism, as shown in Fig. 1, where two planes can evidently be distinguished: the one with the Γ, M, and K high symmetry points and the one above it with A, L, and H points. However, since the main focus in the recent studies of these materials are monolayers, where the reciprocal space is one dimensional and only the Γ M K path is present, while comparing the band structures of monolayers and bulk materials, researchers tend to focus only on the Γ M K path in the bulk as well. However, it seems obvious that there is a high similarity in Γ M K points and A L H points, so they all should be considered in interpretation of the experimental spectra. Recently, Saigal and Ghosh[15] studied bulk MoS_2 by photoreflectance (PR) and have proposed that excitonic transitions at the H point of Brillouin zone are observed ∼30 meV above excitonic transitions at the K point of Brillouin zone. The authors have concluded about such interpretation of PR spectra on the basis of detailed lineshape analysis of PR resonances without theoretical calculations of

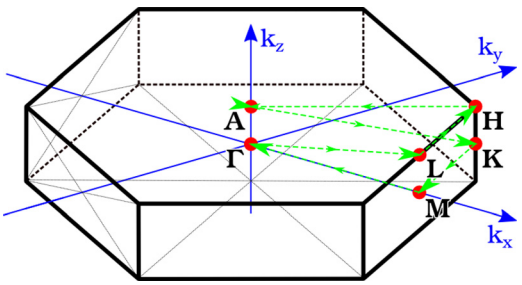

FIG. 1. Brillouin zone of 2H-MX_2 (M = Mo or W and X = S or Se).

[a)]J. Kopaczek and M. P. Polak contributed equally to this work.
[b)]Author to whom correspondence should be addressed. Electronic mail: robert.kudrawiec@pwr.edu.pl

the electronic band structure for this crystal. Previous studies of MoS_2 crystals by modulation spectroscopy[16–19] have not focused on this aspect. Moreover, this issue has never before been studied either experimentally or theoretically for $MoSe_2$, WS_2, and WSe_2 crystals. It is worth noting that the electronic band structure for bulk MoS_2 was reported in many papers, but the H point of Brillouin zone is usually neglected in theoretical analysis, and therefore, it is still unclear how important are optical transitions at this point of Brillouin zone in the interpretation of PR spectra or other differential absorption-like spectra such as contactless electroreflectance (CER) or piezoreflectance (PzR). So far, CER spectroscopy has never been applied to study TMDs but PzR spectroscopy was widely applied to study bulk TMDs.[20–24] However, optical transitions at the H point of Brillouin zone have not been identified in these spectra. It means that the issue of optical transitions at the H point of Brillouin zone is an open question for bulk TMDs, especially that this issue has never been considered for TMDs other than MoS_2 (i.e., $MoSe_2$, WS_2, and WSe_2).

In this work, the electronic band structure for MoS_2, $MoSe_2$, WS_2, and WSe_2 crystals is calculated from the first principles within the density functional theory (DFT) for various points of Brillouin zone including H point. It is clearly shown that the electronic band structure at H point is very symmetric, and hence, a strong optical transition at this point of Brillouin zone is expected in absorption-like spectra. This prediction is confirmed by experimental studies of the electronic band structure of MoS_2, $MoSe_2$, WS_2, and WSe_2 crystals by contactless electroreflectance (CER), photoreflectance, and piezoreflectance, i.e., modulation spectroscopy which is very sensitive to critical points (CP) of Brillouin zone. This paper is organized as follows. In Section II, details on the electronic band structure calculations and CER, PR, and PzR experiments are given. Results of DFT calculations of the electronic band structure for MoS_2, $MoSe_2$, WS_2, and WSe_2 crystals and results of measurements of CER, PR, and PzR spectra for these crystals together with their interpretation and discussion are given in Section III. Conclusions from our studies are summarized in Section IV.

II. METHODS

A. Band structure calculations

The DFT calculations of MoS_2, $MoSe_2$, WS_2, and WSe_2 bulk crystals have been performed with the full-potential linearized augmented plane wave method, as implemented in the WIEN2k code.[25] The van der Waals interactions, very important in geometry optimization of this type of systems, have been included via the DFT-D3 dispersion correction as proposed by Grimme *et al.*[26] used together with generalized gradient approximation (GGA) (PBE) functional.[27] This approach provides an excellent agreement of the geometry optimization with the experimental values (less than 1% of discrepancy), as we have proven in our previous studies[28] where a detailed comparison of different approaches and functionals can be found. To improve the description of the band structure of regular LDA/GGA approach, we have used the modified Becke–Johnson exchange potential with LDA correlation (MBJLDA)[29,30] for all our band structure calculations. This approach has been proven by us to be very effective and efficient numerous times over the years in more traditional III-V semiconductors[31,32] as well as in TMDs in Ref. 28 where a detailed reasoning of this choice is presented. A $10 \times 10 \times 6$ Monkhorst–Pack mesh was used, as a result of convergence studies. The basis set was determined by RKmax equal to 9, and the atomic sphere radii of 2.35, 2.42, 2.02, and 2.3 bohrs were used for Mo, W, S, and Se, respectively.

B. Samples

MoS_2, $MoSe_2$, WS_2, and WSe_2 crystals were grown by iodine assisted vapor transport technique at high temperatures (900–1100 °C) and low pressures ($\sim 1 \times 10^{-6}$ Torr) in a sealed quartz ampoules. During growth at ~50 °C, temperature differential created between hot and cold zones to initiate nucleation and facilitate precursor transport. Prior to growth, quartz ampoules (~15 cm in length, 2.4 cm outer diameter, 2.0 inner diameter) were cleaned in piranha solution and annealed in H_2 gas to remove contaminants. Precursors (Mo, W foils and S, Se nuggets) were mixed in 1:2.05 M:X stoichiometric ratio, and iodine pieces were added as a transport agent. Quartz ampoule is sealed under vacuum (1 μTorr). Samples used to CER, PR, and PzR studies were flakes of macroscopic sizes: $\sim 3 \times 3$ mm in hexagonal plane and thickness <0.2 mm perpendicular to the hexagonal plane. In these measurements, white light reflects at near-normal incidence from the hexagonal plane of the sample.

C. Contactless electroreflectance, photoreflectance, and piezoreflectance measurements

CER, PR, and PzR measurements have been performed in the so-called "bright configuration"[33] where the sample was illuminated by a spectrum of white light from a halogen lamp (150 W) at normal incidence. Next, the light reflected from the sample is dispersed through a 0.55 m focal length single grating monochromator and detected by Si photodiode. The signal measured by photodiode has two components: (i) the DC component which is proportional to I_0R and (ii) the AC component which is proportional to $I_0\Delta R$. The change in the reflectance spectrum (ΔR) appears due to modulation of the built-in electric field (CER and PR measurements) or strain (PzR case) inside the sample. Both DC and AC components are measured with a lock-in amplifier (I_0 is the intensity of reflected light). A computer divides the AC signal by the DC component giving the $\Delta R/R(E)$ spectrum, where E is the photon energy of the incident beam. Phase-sensitive detection of the ΔR signal allows to eliminate the background signal and detect even very weak optical transitions which usually are not observed in the reflectance spectra at room temperature.

For CER measurements, the samples were placed in a capacitor with a half-transparent top electrode made from a copper-wire mesh.[34] They were glued to the bottom copper electrode by a silver paste. The distance between the sample surface and the top electrode was ~0.5 mm. Thus, there is nothing in direct contact with the sample. It means that the sample does not conduct any currents, and the external electric field is able to change the carrier distribution inside the

sample. Note that the main drop in voltage in this system appears in the air gap between the front electrode and the sample. The limit for the applied voltage is the electric breakdown in this air gap. A generator of square AC voltage made in-house was used to generate the AC field inside the capacitor. A maximum peak-to-peak alternating voltage of ∼3.5 kV with the frequency of 280 Hz was used for the modulation.

The pump beam for PR measurements was provided by the 405 nm line of a semiconductor laser. Its intensity was ∼50 mW and diameter on the sample was ∼3 mm. The laser light was chopped by a mechanical chopper with a frequency of 280 Hz.

For PzR measurements, samples were glued on piezoceramics by acrylic glue. AC voltage with an amplitude of 300 V and the frequency of 280 Hz was applied to this piezoceramics in order to modulate strain inside the sample.

The periodic perturbation of the built-in electric field (CER and PR measurements) and strain (piezoreflectance) inside the sample is very small which is the principle of modulation spectroscopy. However, this perturbation is sufficient to slightly change the parameters of an optical transition (its energy, broadening, and intensity) and generate changes in reflectance spectrum which are detected in the lock-in technique.

III. RESULTS AND DISCUSSION

The electronic band structure for MoS_2, $MoSe_2$, WS_2, and WSe_2 crystals calculated from the first principles with the GGA+DFT-D3 geometry optimization and MBJLDA band structure is given in Fig. 2. As mentioned earlier, to properly interpret the transitions observed in experimental measurements, considerations of band structures throughout the whole Brillouin zone, with all the high symmetry points included, are extremely important. Hence, our band structure plots have been calculated along the A → K → M → Γ → L → H → A path, as shown in Fig. 1. The band gap for the four crystals is indirect. Its conduction band minimum and valence band maximum are located at Λ and Γ points, respectively, see Fig. 2. Modulation spectroscopy is not sensitive to indirect optical transitions, so the indirect gap is not probed by CER, PR, or PzR spectroscopy. These techniques are, however, very sensitive to direct optical transitions at critical points of Brillouin zone, and therefore, all points of high symmetry have to be taken into account when the modulated reflectance spectra are analyzed and interpreted.

Probability of an interband transition in absorption ($W_{\vec{k}}$) is given by Fermi's Golden Rule[35,36]

$$W_{\vec{k}} = \frac{2\pi}{\hbar}|\langle\psi_c|H'|\psi_v\rangle|^2\rho_{cv}(\hbar\omega). \quad (1)$$

Here, H′ is the perturbing Hamiltonian for electromagnetic interaction, $\hbar$ is the Planck's constant, ψ_c and ψ_v are the unperturbed wave functions of the conduction and valence band states, respectively, and ρ_{cv} is the joint density of states (JDS) which is given as

$$\rho_{cv}(\hbar\omega) = \frac{1}{4\pi^2}\int_{S(E)}\frac{dS}{|\nabla_k(E_c - E_v)|}, \quad (2)$$

where S(E) is a constant energy surface such as $E = \hbar\omega = E_c - E_v$. For direct optical transitions, a negligible change in the crystal momentum is assumed. Strong optical transitions will appear in modulated reflectance spectra (PzR, PR,

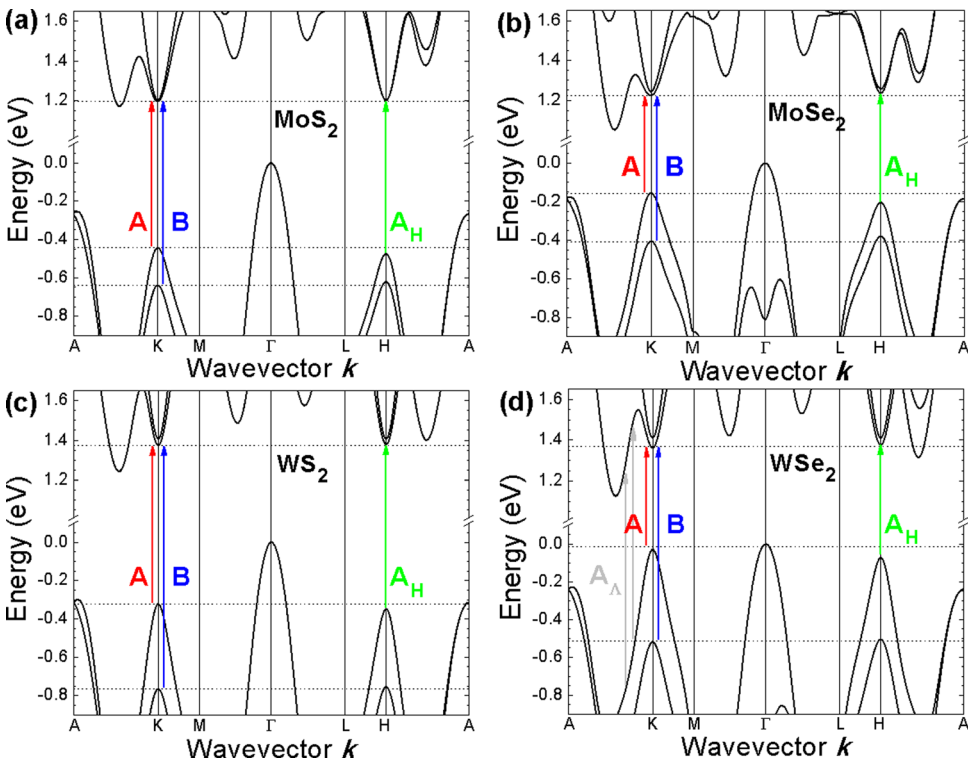

FIG. 2. Electronic band structure of bulk MoS_2 (a), $MoSe_2$ (b), WS_2 (c), and WSe_2 (d) at various points of Brillouin zone. Vertical arrows represent direct optical transitions observed in modulated reflectance spectra.

and CER) at energies where $\nabla_k(E_c - E_v) \approx 0$. Such points are called critical points (CP) and they can be of several types.[37,38] If $\nabla_k E_c = \nabla_k E_c = 0$, we have either a minimum, a maximum, or a saddle point in each band; this usually occurs only at high-symmetry points of Brillouin zone. For TMDs, such conditions are present at the K point of Brillouin zone (see Fig. 2), and therefore, strong A and B transitions are observed in absorption spectra, see for example, absorption spectra for MoS_2 in Refs. 5 and 13. However, very similar conditions are present at the H point of Brillouin zone, see Fig. 2, but optical transitions at these points were not yet identified in absorption spectra measured for these crystals. Regarding the intensity of optical transitions, a direct application of Fermi's Golden Rule to compare this intensity at different CPs of Brillouin zone does not work, especially in modulation spectroscopy where this intensity also depends on the sensitivity of a given CP to the modulated parameter, i.e., this sensitivity will be different for optical transitions at different CPs of Brillouin zone.

According to our calculations, the energy difference between A and A_H transition is rather low and appear in the valence band while the position of conduction band at K and H point is almost the same. For the second valence band (see transition labeled as B in Fig. 2), the difference between valence band maximum at the K and H point is almost negligible for the four crystals. It means that the B and B_H transitions are extremely hard to be resolved in absorption spectra or even in modulated absorption (e.g., PR) which spectrally is more sensitive due to its differential character. However, A and A_H transitions can be distinguished in modulated reflectance spectra and such two transitions were recently identified in PR spectra of MoS_2.[1] In order to study optical transitions at K and H points of Brillouin zone for the four crystals, we applied CER, PR, and PzR spectroscopy. Due to a differential character, the spectral resolution of modulated reflectance is better than the resolution of regular absorption, and therefore, A and A_H transition can be resolved in CER, PR, and PzR spectra.

The left panel in Fig. 3 shows CER, PR, and PzR spectra measured for MoS_2 crystal in the spectral range of A and B transitions at room temperature. In the vicinity of the A transition, two resonances are clearly visible. Two resonances can also be present in the vicinity of B transitions, but they cannot be clearly separated, and therefore, a single resonance is used to simulate ΔR/R spectra in this spectral region.

In order to determine the energies of the optical transitions from CER, PR, and PzR measurements, the ΔR/R spectra were analyzed using the standard CP model.[38] According to this model, a modulated reflectance spectrum can be fitted using the following formula:

$$\frac{\Delta R}{R} = \mathrm{Re}\left[\sum_{j=1}^{n} C_j e^{i\theta_j}(\hbar\omega - E_j + i\Gamma_j)^{-m_j}\right], \tag{3}$$

where n is the number of the spectral functions to be fitted, $\hbar\omega$ is the photon energy of the probe beam, E_j is the CP energy, and Γ_j, C_j, and θ_j are the broadening, amplitude, and phase angle, respectively. The term m_j refers to the type of CPs, i.e., the nature of optical transitions. In this case, we expect excitonic transition even at room temperature due to large exciton binding energy in this material system.[12,39] For such transitions, $m = 2$.

CER, PR, and PzR spectra obtained for MoS_2 crystal can be fitted by three resonances related to excitonic transitions: two at K point (A and B transition) and one at H point (A_H transition). The B_H transition overlaps spectrally with the B transition, and therefore, the two transitions are simulated by a single resonance. Fits of ΔR/R spectra are shown by thick dashed lines in Fig. 3 together with the moduli of the individual CER resonances (ρ), which have been obtained according to Eq. (4)

$$\Delta\rho_j(E) = \frac{|C_j|}{\left[(\hbar\omega - E_j)^2 + \Gamma_j^2\right]^{\frac{m_j}{2}}}, \tag{4}$$

with parameters derived from the fit. The moduli are shown by color thin solid lines in Fig. 3. A comparison of the moduli of individual resonances allows us to evaluate the accuracy of fitting as well as spectral position, broadening, and

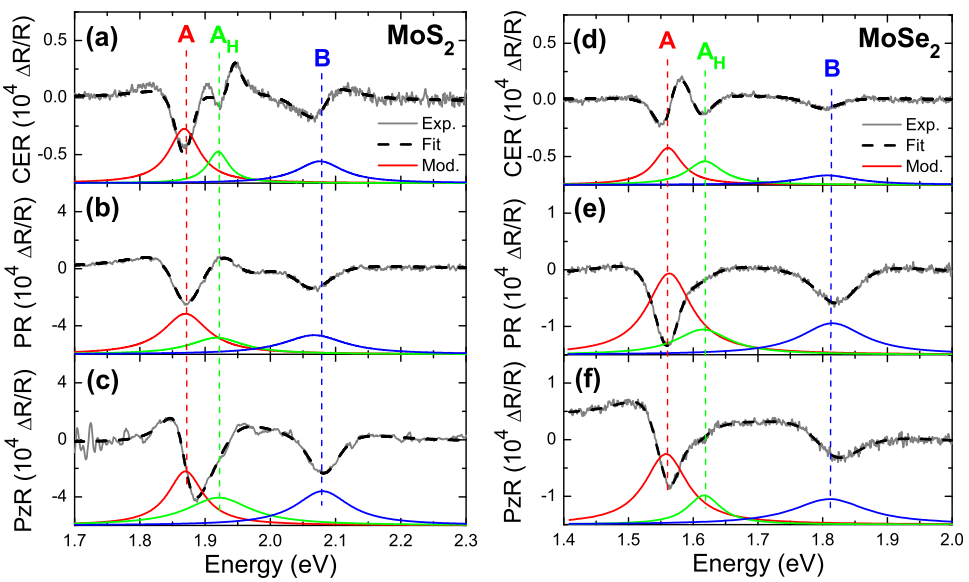

FIG. 3. Room temperature CER, PR, and PzR spectra (grey lines) of bulk MoS_2 (left panel) and $MoSe_2$ (right panel) together with fitting curves (thick dashed lines) and their decomposition for individual moduli of ΔR/R resonances (thin solid color lines).

intensity of individual optical transitions. The most important parameters, i.e., energies of A, A_H, and B transitions, are given in Table I together with the energy separation between these transitions derived from CER, PR, and PzR measurements as well as theoretical predictions. In addition, energies of A, A_H, B, and B_H transitions obtained by PR spectroscopy at low temperatures by Saigal and Ghosh[15] are given in this table. It is visible that the absolute value of energies of optical transitions extracted from modulated reflectance measurements differ a little from theoretical predictions, but it is a rather well known problem in DFT calculations and should be of no concern. The overall shape of the band structure and the relative changes in the band structures should be perfectly correct, since the MBJLDA functional applied in the calculations significantly improves the results over standard LDA/GGA methods.[29,30] It means that the absolute values of energies of direct optical transitions in TMDs can be overestimated but relative changes in the electronic band structure of TMDs (i.e., the energy difference between A and A_H transition) should be, and in fact are, close to experimental data. Taking into account the above argument, we can compare the energy difference between the A and A_H transition obtained from DFT calculations with those derived from modulated reflectance measurements, see Table I. Theoretical prediction gives the value of 33 meV. Experimental data are very close to this value and equal 51, 48, and 51 meV for CER, PR, and PzR measurements. It is worth noting that the energy difference between the B and B_H transition is negative and about twice smaller than the difference between A and A_H transition. Because of this, the two transitions (B and B_H) are not resolved in modulated reflectance. The work made by Saigal and Ghosh was an inspiration to pursue the issue of possible transitions in the other plane of the BZ where the H point is located. The measurements performed there seem to be in excellent quality and agree with both our experimental and theoretical results. Due to the low temperature of their measurements, the authors were also able to distinguish the very spectrally close B and B_H transitions, only about 20 meV apart, which is extremely challenging. However, in light of our current theoretical calculations, the band structures clearly show that the B_H transition should be energetically lower than the B transition, unlike in the case of the A/A_H transitions. Due to the lack of proper theoretical calculations, the authors of Ref. 15 could not predict that fact and seem to misinterpret those transitions, and in fact, the B_H and B transitions should be swapped. This is clearly visible in Table I, where the calculated difference ΔB is negative and the experimental value is nearly identical but the sign is opposite. After careful consideration of both our experimental and theoretical results, we suggest that if a pair of the second, energetically higher, transitions can be distinguished, the first, weaker one should be associated with B_H transition and the second stronger one, higher on the energy scale, is the B transition at K point.

The right panel in Fig. 3 shows CER, PR, and PzR spectra measured for $MoSe_2$ crystal in the spectral range of A and B transitions at room temperature. In this case, an extra A_H transition is also observed besides A and B transitions. According to our DFT calculations, the energy separation between A and A_H transition is about two times larger than in MoS_2 and equals 59 meV. This prediction agrees perfectly with our experimental data, see Table I. B_H transition is still

TABLE I. Energies of A, A_H, B, and B_H transitions obtained from DFT calculations and derived from modulated reflectance measurements. ΔA_{KH} is the energy difference between A_H and A transition, ΔB_{KH} is the energy difference between B_H and A transition, and ΔA_{AB} is the energy difference between A and B transitions.

	A transition (eV)	A_H transition (eV)	ΔA_{KH} (meV)	B transition (eV)	B_H transition (eV)	ΔB_{KH} (meV)	ΔE_{AB} (meV)
MoS_2							
DFT	1.641	1.674	33	1.838	1.821	−17	196
CER	1.869	1.920	51	2.076	NA	NA	207
PR	1.870	1.918	48	2.067	NA	NA	197
PzR	1.870	1.921	51	2.080	NA	NA	210
PR[15]	1.941	1.973	32	2.151	2.171	20	210
$MoSe_2$							
DFT	1.381	1.440	59	1.632	1.616	−16	251
CER	1.561	1.618	57	1.807	NA	NA	246
PR	1.563	1.615	52	1.815	NA	NA	252
PzR	1.558	1.617	59	1.811	NA	NA	253
WS_2							
DFT	1.698	1.729	31	2.140	2.135	−5	442
CER	1.998	2.049	51	2.446	NA	NA	448
PR	1.996	2.048	52	2.438	NA	NA	442
PzR	1.997	2.030	33	2.425	NA	NA	428
WSe_2							
DFT	1.392	1.449	57	1.884	1.882	−2	492
CER	1.650	1.702	52	2.100	NA	NA	450
PR	1.653	1.696	43	2.091	NA	NA	438
PzR	1.656	1.703	47	2.093	NA	NA	437

not clearly resolved in modulated reflectance spectra despite the fact that the energy separation between B and B_H transition is about two times larger than in MoS_2.

CER, PR, and PzR spectra for the remaining two crystals (WS_2 and WSe_2) are shown in Fig. 4. For WS_2 sample, A and A_H transitions are very clearly visible in CER and PR spectrum. In PzR spectrum, they are also visible but they are more weakly resolved. The energy separation between A and A_H transition is close to theoretical prediction (51, 52, and 33 meV vs 31 meV). According to our calculations, B and B_H transitions are basically identical, separated by only −5 and −2 meV (in WS_2 and WSe_2, respectively), and therefore, they are not resolved in modulated reflectance spectra, and a single resonance is used to fit these spectra in this spectral range.

For WSe_2 sample, two resonances are used to fit ΔR/R spectra in the region of A/A_H transitions, and they reproduce experimental data very well. However, it is worth noting that the conduction band in this crystal is significantly splitted at both K and H points. This issue was not commented for previous samples (MoS_2, $MoSe_2$, and WS_2 crystals) since this splitting was small (<2 meV at K point and <3 meV at H point for MoS_2; <18 meV at K point and <22 meV at H point for $MoSe_2$; <32 meV at K point and <27 meV at H point for WS_2). For WSe_2, this splitting equals 49 meV at K point and 35 meV at H point. It means that the optical transition between the top valence band and the second conduction band at the K point of Brillouin zone is expected to be 49 meV above the A transition, and overlaps spectrally with A_H transition. Since modulated reflectance spectra are very well simulated by two resonances in the region of A/A_H transitions, it is rather not justified to use an extra resonance to simulate ΔR/R spectra in this spectral range. However, we have to be aware that the splitting in conduction band leads to extra transitions in modulated reflectance spectra or larger broadening of optical transitions. In the spectral range of B/B_H transition, two resonances are clearly observed in PR spectrum. However, one of them is rather related to an optical transition at band nesting[36] than an optical transition at H point. According to our calculations, the energy difference between B and B_H transition is small (−2 meV), and therefore, a single resonance was used to simulate this transition. For the PR spectrum, an extra resonance has been added to simulate the optical transition at the nesting point of Brillouin zone. According to our calculations of the electronic band structure for this crystal, it could be an optical transition near the K point of the Brillouin zone, see transition labeled as A_Λ in Fig. 2(d). According to our calculations, A_Λ transition is expected to be ∼120–160 meV above the B transition if we neglect excitonic effects. It is very consistent with our experimental data, see PR spectrum in Fig. 4(e), where an overlap between resonances related to B and A_Λ transition is visible and the energy separation between these resonances is ∼110 meV. It is worth noting that band nesting is also present for remaining TMDs, but optical transitions at these points are expected at higher energies than B transitions, and therefore, they are not observed in our ΔR/R spectra in the spectral range discussed in this paper. Optical transitions at band nesting in MoS_2, $MoSe_2$, WS_2, and WSe_2 crystals will be discussed elsewhere.

Summarizing results of modulated reflectance measurements for MoS_2, $MoSe_2$, WS_2, and WSe_2 crystals, it is clear that an extra resonance is observed a few tens of meV above the A transition for all four crystals. This transition can be attributed to a direct optical transition at the H point of Brillouin zone (A_H transition), since a significant critical point is expected there, according to our DFT calculations. In addition, a B_H transition is expected at almost the same energy as the B transition, but the two transitions are not resolved in our modulated reflectance spectra due to this small energy separation between them. The small energy separation between optical transitions at K and H point can be the reason why the optical transitions at H point of Brillouin zone are usually neglected when the optical absorption spectra are analyzed. The other reason can be excited states of excitonic transitions. They are usually expected also a few tens of meV above A and B transitions which may cause the confusion. In general, a signal which could be

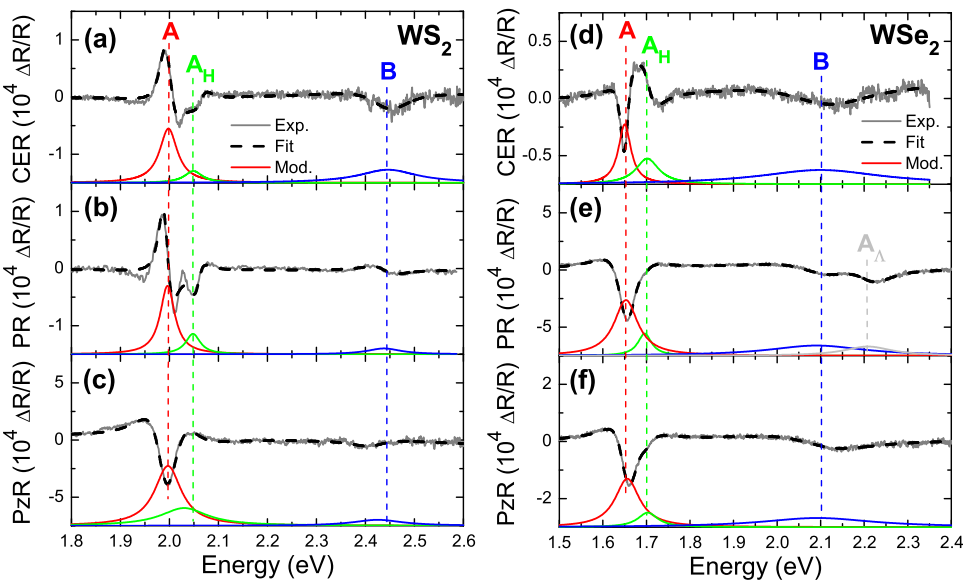

FIG. 4. Room temperature CER, PR, and PzR spectra (grey lines) of bulk WS_2 (left panel) and WSe_2 (right panel) together with fitting curves (thick dashed lines) and their decomposition for individual moduli of ΔR/R resonances (thin solid color lines).

related to excited states of A and B excitonic transition can be present in ΔR/R spectra, but the A_H resonances we observe are too strong to be attributed to an excited state of the A exciton. We expect that ΔR/R signal, which could be related to excited states of A excitonic transition, is very weak at room temperature, and therefore, such transition can be neglected in our analysis of ΔR/R signal while the A_H transition is relatively strong due to the presence of a critical point at the H point of Brillouin zone very similar to the one at the K point of Brillouin zone. Therefore, optical transitions at the H point of Brillouin zone are observed in ΔR/R spectra, besides optical transitions at K point.

IV. CONCLUSIONS

It has been shown that the electronic band structure at the H point of Brillouin zone is very symmetric and similar to the electronic band structure at K point, and therefore, direct optical transitions at H point should be expected in modulated reflectance spectra besides direct optical transitions at K point of Brillouin zone. The direct optical transition at H point (A_H transition) has been observed a few tens of meV above the A transition in CER, PR, and PzR spectra for the four crystals. The second transition at the H point of Brillouin zone (B_H transition) overlaps spectrally with the B transition at the K point, and therefore, an extra resonance which could be related to the B_H transition is not resolved in modulated reflectance spectra at room temperature. However, the theoretical calculations show that the B_H transition should be expected for slightly lower energies than the B transition, in contrast to A_H and A, which is especially important in MoS_2 where the B-B_H separation is the largest. The spectral difference between A and A_H transitions has been found to be in a very good agreement with theoretical predictions.

ACKNOWLEDGMENTS

The DFT calculations were performed in the Wroclaw Centre for Networking and Supercomputing. M.P.P. acknowledges the support within the "Diamond Grant" (DI2013 006143) from the MNiSzW.

[1]Q. Tang and A. Zhou, "Graphene-analogous low-dimensional materials," Prog. Mater. Sci. **58**, 1244 (2013).
[2]H. Wang, H. Yuan, S. S. Hong, Y. Li, and Y. Cui, "Physical and chemical tuning of two-dimensional transition metal dichalcogenides," Chem. Soc. Rev. **44**, 2664 (2015).
[3]T. Heine, "Transition metal chalcogenides: ultrathin inorganic materials with tunable electronic properties," Acc. Chem. Res. **48**, 65 (2015).
[4]J. A. Wilson and A. D. Yoffe, "The transition metal dichalcogenides discussion and interpretation of the observed optical, electrical and structural properties," Adv. Phys. **18**, 193 (1969).
[5]A. R. Beal, J. C. Knights, and W. Y. Liang, "Transmission spectra of some transition metal dichalcogenides. II. Group VIA: trigonal prismatic coordination," J. Phys. C: Solid State Phys. **5**, 3540 (1972).
[6]L. F. Mattheiss, "Band structures of transition-metal-dichalcogenide layer compounds," Phys. Rev. B **8**, 3719 (1973).
[7]R. V. Kasowski, "Band structure of MoS_2 and NbS_2," Phys. Rev. Lett. **30**, 1175 (1973).
[8]R. Coehoorn, C. Haas, J. Dijkstra, C. J. F. Flipse, R. A. de Groot, and A. Wold, "Electronic structure of $MoSe_2$, MoS_2, and WSe_2. I. Band-structure calculations and photoelectron spectroscopy," Phys. Rev. B **35**, 6195 (1987).
[9]R. Mamy, A. Boufelja, and B. Carricaburu, "Angle resolved photoemission and electronic band structure of MoS_2," Phys. Status Solidi B **141**, 467 (1987).
[10]K. Fives, I. T. McGovern, R. McGrath, R. Cimino, G. Hughes, A. McKinley, and G. Thornton, "The photoelectron bandstructure of molybdenum disulphide," J. Phys.: Condens. Matter **4**, 5639 (1992).
[11]K. Kobayashi and J. Yamauchi, "Electronic structure and scanning-tunneling-microscopy image of molybdenum dichalcogenide surfaces," Phys. Rev. B **51**, 17085 (1995).
[12]T. Cheiwchanchamnangij and W. R. L. Lambrecht, "Quasiparticle band structure calculation of monolayer, bilayer, and bulk MoS_2," Phys. Rev. B **85**, 205302 (2012).
[13]A. Molina-Sanchez, D. Sangalli, K. Hummer, A. Marini, and L. Wirtz, "Effect of spin-orbit interaction on the optical spectra of single-layer, double-layer, and bulk MoS_2," Phys. Rev. B **88**, 045412 (2013).
[14]R. Roldán, J. A. Silva-Guillén, M. Pilar López-Sancho, F. Guinea, E. Cappelluti, and P. Ordejón, "Electronic properties of single-layer and multilayer transition metal dichalcogenides MX_2 (M = Mo, W and X = S, Se)," Ann. Phys. (Berlin) **526**, 347 (2014).
[15]N. Saigal and S. Ghosh, "H-point exciton transitions in bulk MoS_2," Appl. Phys. Lett. **106**, 182103 (2015).
[16]J. Bordas and E. A. Davi, "Electromodulation spectroscopy of excitons: molybdenum disulphide," Phys. Status Solidi B **60**, 505 (1973).
[17]E. Fortin and F. Raga, "Excitons in molybdenum disulphide," Phys. Rev. B **11**, 905 (1975).
[18]H. Meinhold and G. Weiser, "Modulation spectroscopy on MoS_2, and $MoSe_2$," Phys. Status Solidi B **73**, 105 (1976).
[19]K. Saiki, M. Yoshimi, and S. Tanaka, "Modulation spectroscopy on the group IV and VI transition-metal dichalcogenides," Phys. Status Solidi B **88**, 607 (1978).
[20]K. K. Tiong, T. S. Shou, and C. H. Ho, "Temperature dependence piezoreflectance study of the effect of doping MoS_2 with rhenium," J. Phys.: Condens. Matter **12**, 3441 (2000).
[21]P. C. Yen, H. P. Hsu, Y. T. Liu, Y. S. Huang, and K. K. Tiong, "Temperature dependences of energies and broadening parameters of the band-edge excitons of Re-doped WS_2 and 2H-WS_2 single crystals," J. Phys.: Condens. Matter **16**, 6995 (2004).
[22]D. O. Dumcenco, H. P. Hsu, Y. S. Huang, C. H. Liang, K. K. Tiong, and C. H. Du, "Optical properties of tungsten disulfide single crystals doped with gold," Mater. Chem. Phys. **111**, 475 (2008).
[23]Y. J. Wu, P. H. Wu, J. Jadczak, Y. S. Huang, C. H. Ho, H. P. Hsu, and K. K. Tiong, "Piezoreflectance study of near band edge excitonic-transitions of mixed-layered crystal $Mo(S_xSe_{1-x})_2$ solid solutions," J. Appl. Phys. **115**, 223508 (2014).
[24]M. Sigiro, Y.-S. Huang, Ch.-H. Ho, Y.-Ch. Lin, and K. Suenaga, "Influence of rhenium on the structural and optical properties of molybdenum disulfide," Jpn. J. Appl. Phys., Part 1 **54**, 04DH05 (2015).
[25]P. Blaha, K. Schwarz, G. Madsen, D. Kvasnicka, and J. Luitz, *WIEN2k, An Augmented Plane Wave + Local Orbitals Program for Calculating Crystal Properties* (Karlheinz Schwarz, Techn. Universität Wien, Austria, 2001).
[26]S. Grimme, J. Antony, S. Ehrlich, and H. Krieg, "A consistent and accurate ab initio parametrization of density functional dispersion correction (DFT-D) for the 94 elements H-Pu," J. Chem. Phys. **132**, 154104 (2010).
[27]J. P. Perdew, K. Burke, and M. Ernzerhof, "Generalized gradient approximation made simple," Phys. Rev. Lett. **77**, 3865 (1996).
[28]F. Dybała, M. Polak, J. Kopaczek, P. Scharoch, S. Tongay, and R. Kudrawiec, "Pressure coefficients for direct optical transitions in MoS_2, $MoSe_2$, WS_2, and WSe_2 crystals and semiconductor to metal transition," Sci. Rep. **6**, 26663 (2016).
[29]F. Tran and P. Blaha, "Accurate band gaps of semiconductors and insulators with a semilocal exchange-correlation potential," Phys. Rev. Lett. **102**, 226401 (2009).
[30]J. A. Camargo-Martínez and R. Baquero, "Performance of the modified Becke-Johnson potential for semiconductors," Phys. Rev. B **86**, 195106 (2012).
[31]M. P. Polak, P. Scharoch, and R. Kudrawiec, "First-principles calculations of bismuth induced changes in the band structure of dilute Ga–V–Bi and In–V–Bi alloys: chemical trends versus experimental data," Semicond. Sci. Technol. **30**, 094001 (2015).
[32]M. P. Polak, P. Scharoch, R. Kudrawiec, J. Kopaczek, M. J. Winiarski, W. M. Linhart, M. K. Rajpalke, K. M. Yu, T. S. Jones, M J. Ashwin, and

T. D. Veal, "Theoretical and experimental studies of electronic band structure for $GaSb_{1-x}Bi_x$ in the dilute Bi regime," J. Phys. D **47**, 355107 (2014).
[33]R. Kudrawiec and J. Misiewicz, "Photoreflectance and contactless electroreflectance measurements of semiconductor structures by using bright and dark configurations," Rev. Sci. Instrum. **80**, 096103 (2009).
[34]R. Kudrawiec, "Application of contactless electroreflectance to III-nitrides," Phys. Status Solidi B **247**, 1616 (2010).
[35]M. Grundmann, *The Physics of Semiconductors: An Introduction Including Nanophysics and Applications* (Springer-Verlag, Berlin, Germany, 2006).
[36]A. Carvalho, R. M. Ribeiro, and A. H. C. Neto, "Band nesting and the optical response of two-dimensional semiconducting transition metal dichalcogenides," Phys. Rev. B **88**, 115205 (2013).
[37]F. Bassani and G. Pastori Parravicini, *Electronic States and Optical Transitions in Solids* (Pergamon Press, 1975).
[38]D. E. Aspnes, "Third-derivative modulation spectroscopy with low-field electroreflectance," Surf. Sci. **37**, 418 (1973).
[39]T. Goto, Y. Kato, K. Uchida, and N. Miura, "Exciton absorption spectra of MoS_2 crystals in high magnetic fields up to 150 T," J. Phys.: Condens. Matter **12**, 6719 (2000).